

## High-pressure Raman-scattering study of germanium diselenide

Z. V. Popović and Z. Jakšić  
*Institute of Physics, P.O. Box 57, 11001 Belgrade, Yugoslavia*

Y. S. Raptis and E. Anastassakis  
*Physics Department, National Technical University, 15780 Athens, Greece*  
 (Received 22 May 1997)

We have measured the Raman-scattering spectra of the  $\beta$  modification of  $\text{GeSe}_2$  at low temperatures and under hydrostatic pressures up to 8 GPa at room temperature. A total of 28 modes of symmetry  $A_g$  and 29 of symmetry  $B_g$  were resolved by polarized light-scattering measurements at 10 K. The mode frequencies harden with pressure up to 2.5 GPa. At 6.2 GPa the changes of the spectra reveal a transition to an amorphous phase. Further increase of the pressure up to 7 GPa yields strong indication of a phase transition from the disordered phase to the low-temperature modification of  $\text{GeSe}_2$ . At 8 GPa, this modification transforms back to the disordered phase. All these phase transformations are reversible. [S0163-1829(98)05802-0]

### I. INTRODUCTION

Depending on growth temperature, germanium diselenide appears in three crystallographic modifications: the low-temperature (LT, $\alpha$ )- $\text{GeSe}_2$  with a complex three-dimensional crystal structure;<sup>1</sup> the high-temperature (HT, $\beta$ )- $\text{GeSe}_2$  with layered structure;<sup>2</sup> the  $\gamma$ - $\text{GeSe}_2$  modification with a structure similar to that of  $\text{SnSe}_2$ .<sup>3</sup> The basic building blocks of the  $\text{GeSe}_2$  structure are  $\text{GeSe}_4$  tetrahedra which in the LT phase are mutually connected only via common corners, and in the HT modification both via common corners and via common edges. The schematic network connection of  $\alpha$ - and  $\beta$ - $\text{GeSe}_2$  is shown in Fig. 1. In addition to the crystalline modifications, the glassy or amorphous  $\text{GeSe}_2$  ( $a$ - $\text{GeSe}_2$ ) consists of  $\text{GeSe}_4$  tetrahedral units connected to each other in different corner-sharing and edge-sharing patterns.

The vibrational properties of the HT modification have already been investigated through infrared (IR) and Raman-scattering spectroscopy.<sup>4,5</sup> The unit cell of this modification contains two layers with eight molecular units each. Due to the very complex crystal structure and the low symmetry of the corresponding space group ( $P2_1/c$ ), the full assignment of the expected large number of optical phonons (72 Raman active, 69 IR active) has not been completed yet. Recently, the most intense Raman bands of the LT and HT phases have been assigned using a simple valence-force-field model combined with a bond polarizability model.<sup>6,7</sup> It has been shown<sup>6</sup> that the highest intensity modes of the LT phase (at  $201\text{ cm}^{-1}$ ) and of the HT phase (at  $211\text{ cm}^{-1}$ ) represent  $A_1$  in-phase vibrations of corner-sharing  $\text{GeSe}_4$  tetrahedra. In the HT phase, very close to this mode at  $\sim 216\text{ cm}^{-1}$ , there appears an  $A_1$  mode representing an in-phase vibration of edge-sharing  $\text{GeSe}_4$  tetrahedra.

The vibrational properties of amorphous  $\text{GeSe}_2$  have been studied in detail using Raman-scattering spectroscopy.<sup>8-15</sup> The highest intensity Raman band at  $199\text{ cm}^{-1}$  represents  $A_1$  in-phase breathing vibration extended along the corner-sharing  $\text{GeSe}_4$  tetrahedral chain structure. The companion mode ( $A_{1c}$ ) at  $216\text{ cm}^{-1}$  is related to breathinglike motions of Se about the edge-sharing link of the basic tetrahedral

units.<sup>10</sup> Two additional bands at about  $175$  and  $257\text{ cm}^{-1}$  originate from Ge-Ge and Se-Se vibrations, respectively.<sup>8,12</sup> These vibrations are absent in all crystalline modifications. The above assignments of the vibrational modes in amorphous  $\text{GeSe}_2$  have been supported by a recent *ab initio* molecular-dynamics study of glassy  $\text{GeSe}_2$ .<sup>13</sup>

Raman-scattering spectra of amorphous and single-crystal germanium dichalcogenides at high pressures have been presented in Refs. 15, 16. As shown in Ref. 15, there is no change in the frequencies of the  $A_1$  and  $A_{1c}$  modes in  $a$ - $\text{GeSe}_2$  up to 2 GPa. In the case of the  $\text{GeSe}_2$  single crystal, as the pressure increases to 5 GPa, a splitting appears of the highest intensity mode at  $211\text{ cm}^{-1}$ .

In this work we report Raman-scattering measurements of the  $\beta$  modification of  $\text{GeSe}_2$  at low temperatures (10 K) using polarized light. The  $A_g$  and  $B_g$  symmetry modes are identified. Furthermore, unpolarized spectra were taken under hydrostatic pressures up to 8 GPa at room temperature. We observed that as the pressure increases, the layered structure of HT  $\text{GeSe}_2$  undergoes a transformation first into a fully disordered structure and then into the LT modification; further pressure increase leads to amorphization. These phase transformations are found to be reversible.

### II. EXPERIMENTAL DETAILS

Single crystals of HT  $\text{GeSe}_2$  were grown using a standard Bridgman technique. Details of the growth process have been published elsewhere.<sup>4</sup> The resulting single crystals could be readily cleaved to produce optical quality surface areas of several  $\text{mm}^2$ . Only freshly cleaved surfaces were used in our Raman-scattering measurements.

The hydrostatic pressure measurements for pressures up to 9 GPa were taken using a gasketed diamond-anvil-cell (DAC), with a methanol-ethanol mixture as pressure transmitting fluid. The pressures were determined using the ruby luminescence. All spectra under pressure were measured in the backscattering geometry using the  $514.5\text{ nm}$ /Ar laser line

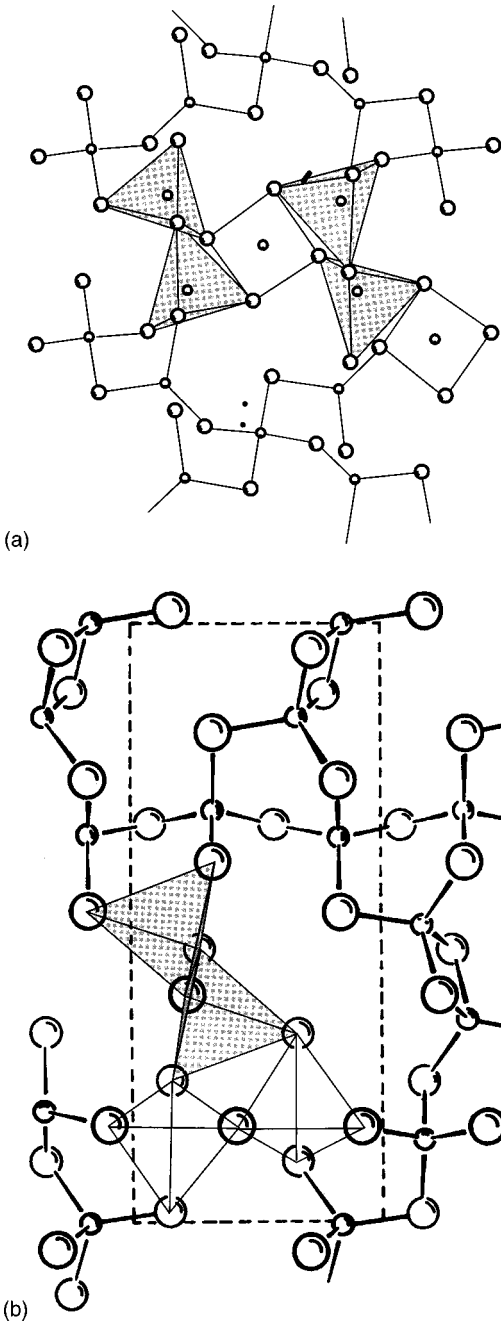


FIG. 1. Atomic arrangements in LT (a) and HT (b) modifications of  $\text{GeSe}_2$ . Small circles denote Ge atoms, large Se atoms.

for excitation and were unpolarized. The laser power was 25 mW.

### III. RESULTS

Raman-scattering spectra of HT  $\text{GeSe}_2$  in the 5–355  $\text{cm}^{-1}$  spectral range at  $T=10$  K are presented in Fig. 2. The upper spectrum (a) was taken with parallel polarizations and corresponds to the  $A_g$  modes, while the  $B_g$  modes are shown in the lower spectrum taken with crossed polarizations (b). The frequencies of all modes observed are collected in Table I.

Raman spectra at different hydrostatic pressures are shown in Figs. 3 and 4; the spectrum (a) of Fig. 3 was taken

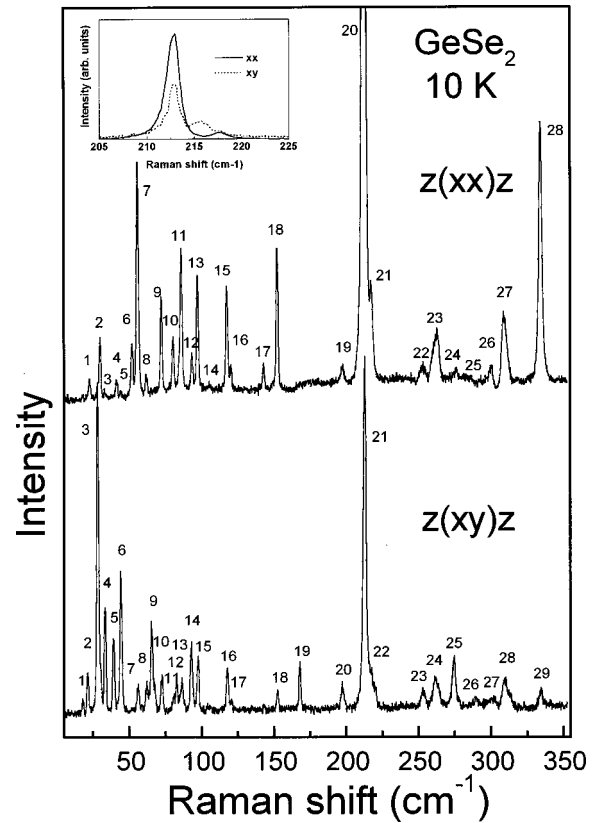


FIG. 2. Polarized Raman spectra of HT  $\text{GeSe}_2$  at 10 K. Inset: Polarized spectra in the vicinity of the highest intensity mode.

with the sample placed inside the DAC without pressure transmitting fluid, to insure genuine  $P=0$  conditions. Below the highest intensity mode at about  $211 \text{ cm}^{-1}$ , we observe bond-bending modes at  $\sim 30, 72, 85, 97,$  and  $117 \text{ cm}^{-1}$ , while high-frequency modes at  $251, 258, 305,$  and  $329 \text{ cm}^{-1}$  are clearly observable. Increasing of the pressure causes an increase of all frequencies, as shown collectively in Fig. 5. Figure 3(d) shows a broadening of the highest intensity mode, at  $\sim 2.5$  GPa, which is a precursor of the splitting shown clearly at 3.8 GPa. At a pressure of 5.2 GPa a number of defects is produced in the structure and the pronounced splitting is absorbed into a broad background representing the phonon density of states of amorphous  $\text{GeSe}_2$ .<sup>13</sup> Further increase in pressure results in the appearance of a broad mode at  $\sim 200 \text{ cm}^{-1}$ ; its well resolved structure is clearly seen between 6.2 and 6.9 GPa, Figs. 4(a) and 4(b). Further increase in pressure leads to a narrowing of this mode. Upon lowering the pressure we observe [Figs. 4(e)–4(g)] full reversibility of the structural transformations.

### IV. DISCUSSION

Factor-group analysis of  $\beta\text{-GeSe}_2$  (space group  $P2_1/c$ ) predicts  $36 A_g + 36 B_g$  modes. In the present case<sup>5</sup> (where the twofold axis lies on the  $ab$ -layer plane, along crystallographic axis  $y$ ) ( $C_2^y \parallel \mathbf{b}$ ), the  $A_g$  modes may be observed for parallel ( $xx, yy, zz$ ) and crossed ( $xz$ ) polarizations, while the  $B_g$  modes are observed for crossed polarizations ( $xy, yz$ ). There are 28  $A_g$  and 29  $B_g$  symmetry modes confirmed from the spectra of Fig. 2 and Table I. Being of low intensity, the

TABLE I. Phonon frequencies (in  $\text{cm}^{-1}$ ) of Raman-active modes of  $\text{GeSe}_2$  at 10 K. The  $A_g$  and  $B_g$  symmetry modes are those in Figs. 2(a) and 2(b), respectively.

No. of peaks	$A_g$	$B_g$
1	22.8	18.0
2	30.0	21.3
3	32.9	28.1
4	41.2	33.1
5	44.2	38.9
6	51.9	44.1
7	55.7	56.0
8	62.0	62.1
9	72.0	65.1
10	80.0	72.4
11	85.7	80.7
12	93.2	82.5
13	97.1	86.2
14	105.2	92.7
15	117.0	97.4
16	120.4	117.6
17	143.0	120.6
18	152.3	152.2
19	198.0	168.0
20	212.6	197.3
21	217.3	213.0
22	253.2	215.4
23	262.5	253.0
24	276.0	261.5
25	282.3	274.6
26	300.2	289.3
27	308.8	300.2
28	334.2	309.4
29		334.6

missing modes are probably below the noise level and/or are masked by the modes of high intensity. To further examine this assumption, we have taken and show in the inset of Fig. 2 the  $205\text{--}225\text{ cm}^{-1}$  spectral range; two modes are observed in the vicinity of the highest intensity mode, which can be experimentally resolved; one of them is of  $A_g$  symmetry ( $217.3\text{ cm}^{-1}$ ), the other of  $B_g$  symmetry ( $215.4\text{ cm}^{-1}$ ). According to the lattice-dynamical calculations of Ref. 6, five modes (those assigned by numbers 43–48 in Ref. 6) should be expected in the vicinity of the highest intensity mode, between  $211$  and  $216\text{ cm}^{-1}$  (300 K). Only three modes can be observed in our spectra at 10 K, measured with a resolution of  $0.5\text{ cm}^{-1}$ .

In layered structure materials, the most common modes are those originating from vibrations of rigid layers, against each other. These modes are called rigid-layer (RL) modes and appear at very low frequencies. As discussed earlier,<sup>4</sup> there are two shear RL modes ( $B_g$  symmetry) and one compressional RL mode ( $A_g$  symmetry). According to Fig. 2, candidates for RL modes are those at  $18$  and  $21.3$  ( $B_g$ ) and  $22.8\text{ cm}^{-1}$  ( $A_g$ ), while the modes at  $28.1$  ( $B_g$ ),  $30$  ( $A_g$ ), and  $33.1$  ( $B_g$ ) correspond to low-lying optical modes as they have their own IR counterparts.<sup>5</sup> Other modes, in the spectral range from  $30$  to  $150\text{ cm}^{-1}$ , are the bond-bending vibrations,

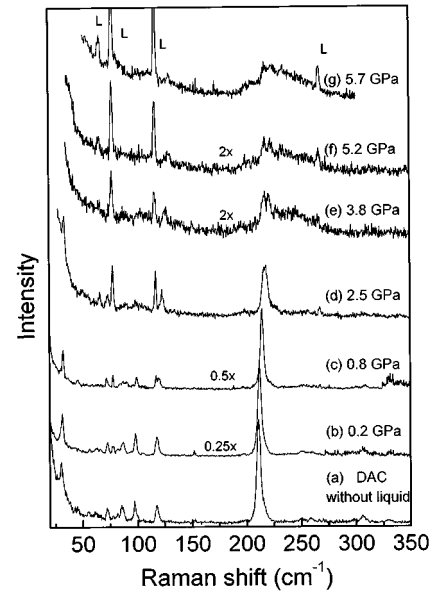


FIG. 3. Unpolarized Raman spectra of  $\text{GeSe}_2$  at different hydrostatic pressures showing the phase change from HT- $\text{GeSe}_2$  to  $a$ - $\text{GeSe}_2$ .

while those above  $200\text{ cm}^{-1}$  are identified as bond-stretching vibrations.

As can be seen from Fig. 2 and Table I there are some  $A_g$  and  $B_g$  symmetry phonon lines which appear at nearly equal frequencies. Because the polarized spectrum ( $A_g$ ) was one order of magnitude stronger in intensity than that of the depolarized ones ( $B_g$ ), it is reasonable to expect some leakage of  $A_g$  symmetry modes in the depolarized configuration. As both the highest intensity modes of  $A_g$  symmetry in the bond-bending spectral region (modes denoted by 7 and 11) and the highest intensity mode (denoted by 20) in the bond-stretching region have no counterparts in the same positions of the  $B_g$  spectrum, we conclude that no polarization leakage

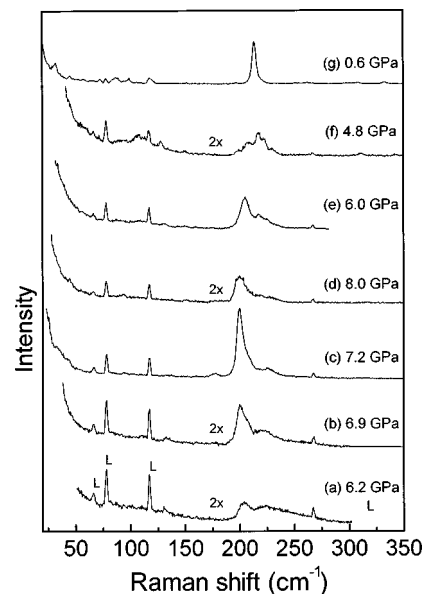


FIG. 4. Unpolarized Raman spectra of  $\text{GeSe}_2$  at different hydrostatic pressures showing the phase change from  $a$ - $\text{GeSe}_2$  to LT- $\text{GeSe}_2$ , to  $a$ - $\text{GeSe}_2$  (upstroke) and back to HT- $\text{GeSe}_2$  (downstroke).

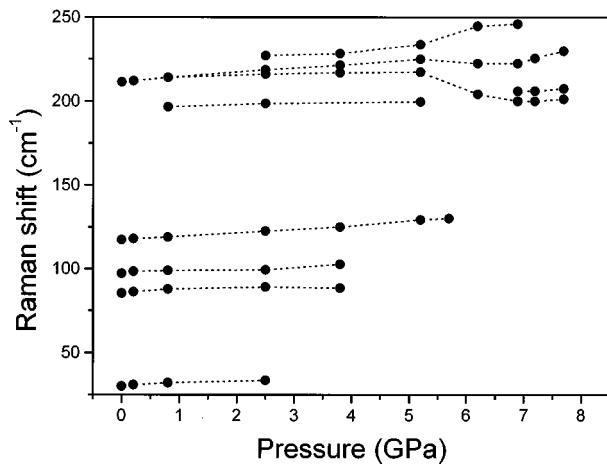


FIG. 5. Pressure dependence of selected mode frequencies of GeSe<sub>2</sub>.

exists in Fig. 2. The appearance of some modes at almost the same frequencies is a consequence of symmetry similarity of the normal modes and the appearance of many such modes in a narrow spectral range.

Ambient pressure measurements, shown in Fig. 3(a) coincide with the polarized Raman spectra of Fig. 2(a). Thus, the high-pressure Raman spectra presented here are limited to the  $A_g$  symmetry modes only. A shift in mode frequency with pressure up to 4 GPa is evident for most of the modes, as shown in Fig. 5. At higher pressure, all modes, except those at  $\sim 219$  and  $126 \text{ cm}^{-1}$ , are of too low intensity to be distinguished from the level of noise. Our study, therefore, is mainly focused on the bond-stretching modes. The shift rate of the  $A_1$  mode frequency for pressures up to 2 GPa is  $2 \text{ cm}^{-1}/\text{GPa}$ . Further increase in pressure resulted in a splitting of the highest intensity mode. As shown in the inset of Fig. 2, the highest intensity mode represents a superposition of at least two modes; one of them represents an  $A_1$  vibration of corner-sharing GeSe<sub>4</sub> tetrahedra while the other,  $A_{1c}$ , represents an  $A_1$  vibration of edge-sharing GeSe<sub>4</sub> tetrahedra. At room temperature, no splitting of these modes is observed, because they appear at very close frequencies, while the intensity of the  $A_{1c}$  mode is very weak compared to that of the  $A_1$  vibration. With an increase of pressure up to 2.5 GPa, these two modes become equal in intensity, as indicated by the noticeable splitting of the highest intensity mode into a doublet. The presence of two modes becomes more evident with further pressure increase: all other modes, except the one at  $126 \text{ cm}^{-1}$  (3.8 GPa), disappear into the noise level. In addition, laser plasma lines at  $\sim 66, 77, 117,$  and  $267 \text{ cm}^{-1}$  (denoted by  $L$  in Figs. 3, 4) appear and mask the signal. Further pressure increase up to 5.2 GPa causes so many defects in the structure that no sharp peaks are present; instead a broad maximum reflecting phonon density of states sets in. At this pressure, a slight increase in intensity of a mode at  $\sim 200 \text{ cm}^{-1}$  is also observed. Further pressure increase to 5.7 GPa leads to two broad modes at  $\sim 200$  and  $225 \text{ cm}^{-1}$ . The shape and frequency of these modes correspond to that of amorphous GeSe<sub>2</sub>. This means that a pressure of  $\sim 6$  GPa causes complete breakdown of the crystal structure and formation of a disordered state. Bearing in mind that the mode

of amorphous GeSe<sub>2</sub> at  $200 \text{ cm}^{-1}$  represents vibrations of corner-sharing GeSe<sub>4</sub> tetrahedra and the mode at  $225 \text{ cm}^{-1}$  vibrations of edge-sharing GeSe<sub>4</sub> tetrahedra, we conclude that the structure of GeSe<sub>2</sub> at 6.2 GPa corresponds to that of amorphous GeSe<sub>2</sub>.

We were not able to clearly resolve the mode at  $175 \text{ cm}^{-1}$ , which in amorphous GeSe<sub>2</sub> represents Ge-Ge vibrations, and the one at  $257 \text{ cm}^{-1}$  which represents Se-Se vibrations. This is an indication that the structure of GeSe<sub>2</sub> at 6.2 GPa, although completely disordered, is not identical to amorphous GeSe<sub>2</sub>. An abrupt increase in intensity of the  $200 \text{ cm}^{-1}$  mode with further pressure rise, probably originates from an increase in concentration of clusters with corner-sharing GeSe<sub>4</sub> tetrahedra. Further ordering of the structure is observed at a pressure of 7.2 GPa, as reflected by an increase in intensity of the  $200 \text{ cm}^{-1}$  mode and the narrowing of its fullwidth at half maximum ( $= 6 \text{ cm}^{-1}$ ). In addition, the elastically scattered light at low frequencies decreases suggesting also ordering of the structure at these pressures.

The presence of the modes at about 200 and  $206 \text{ cm}^{-1}$  leads to the conclusion that the newly formed structure is an LT modification of GeSe<sub>2</sub>, i.e., a modification consisting of corner-sharing GeSe<sub>4</sub> tetrahedra only. This means that at  $\sim 7$  GPa, the disordered (amorphous) GeSe<sub>2</sub> structure is transformed into the LT modification with a three-dimensional structure. Similar transition from the amorphous to the LT modification of GeSe<sub>2</sub> can be obtained also by photoinduced crystallization.<sup>12,14</sup> Namely, it is known that when amorphous GeSe<sub>2</sub> is illuminated by an argon-laser beam of an intensity below 10 mW, no structural transformation occurs. However, if the beam intensity is 15 mW, the transition from the amorphous to the LT phase takes place. Further increase in the intensity transforms the LT phase into a HT one. This change is not, however, an abrupt one. The transition from amorphous to the LT or HT phase proceeds via a microcrystal phase. According to the spectra of Fig. 4, a similar transition occurs in the present case, namely at 7.2 GPa the LT phase is not a pure one, for there is a phase of edge-sharing tetrahedra confirmed by the  $225 \text{ cm}^{-1}$  mode. Further pressure increase leads to broadening of the  $200 \text{ cm}^{-1}$  mode, revealing a less ordered structure and a tendency of the sample to return to the amorphous state.

As the pressure is decreased, the structural changes do not occur at the same pressures as in the up stroke. Thus, at 6 GPa both the LT as well as the HT phase, that is a mixed phase, are recorded. Only at the reduced pressure of  $\sim 0.6$  GPa, does a complete reconstruction of the HT modification occur, Fig. 4(g).

In conclusion, we observed that, as the pressure increases, the HT modification of GeSe<sub>2</sub> undergoes a transformation first into a fully disordered structure, and then into the LT modification; further pressure increase leads to amorphization. All these phase transformations are reversible.

#### ACKNOWLEDGMENTS

This work was supported by the Serbian Ministry of Science and Technology under Project No. 01E09, and by National Technical University, Athens.

- <sup>1</sup>G. von Dittmar and H. Schäfer, *Acta Crystallogr., Sect. B: Struct. Crystallogr. Cryst. Chem.* **32**, 1188 (1976).
- <sup>2</sup>G. von Dittmar and H. Schäfer, *Acta Crystallogr., Sect. B: Struct. Crystallogr. Cryst. Chem.* **32**, 2726 (1976).
- <sup>3</sup>D. I. Bletskan, V. S. Gerasimenko, and M. Yu. Sichka, *Kristallografiya* **24**, 83 (1979).
- <sup>4</sup>Z. V. Popovic and H. J. Stolz, *Phys. Status Solidi B* **108**, 153 (1981).
- <sup>5</sup>Z. V. Popovic and R. Gajic, *Phys. Rev. B* **33**, 5878 (1986).
- <sup>6</sup>K. Inoue, O. Matsuda, and K. Murase, *Solid State Commun.* **79**, 905 (1991).
- <sup>7</sup>K. Inoue, O. Matsuda, and K. Murase, *Physica B* **219&220**, 520 (1996).
- <sup>8</sup>P. M. Bridenbaugh, G. P. Espinosa, J. C. Phillips, and J. P. Remeka, *Phys. Rev. B* **20**, 4140 (1979).
- <sup>9</sup>R. J. Nemanich, F. L. Galeener, J. C. Mikkelsen, Jr., G. A. N. Connel, G. Etherington, A. C. Wright, and R. N. Sinclair, *Physica B & C* **117B&118B**, 959 (1983).
- <sup>10</sup>K. Inoue, O. Matsuda, and K. Murase, *J. Non-Cryst. Solids* **150**, 197 (1992).
- <sup>11</sup>J. A. Aranovitz, J. R. Banavar, M. A. Marcus, and J. C. Phillips, *Phys. Rev. B* **28**, 4454 (1983).
- <sup>12</sup>S. Sugai, *Phys. Rev. Lett.* **57**, 456 (1986); *Phys. Rev. B* **35**, 1345 (1987).
- <sup>13</sup>M. Cobb, D. A. Drabold, and R. L. Cappelletti, *Phys. Rev. B* **54**, 12 162 (1996).
- <sup>14</sup>E. Haro, Z. S. Xu, J. F. Morhange, M. Balkanski, G. P. Espinosa, and J. C. Phillips, *Phys. Rev. B* **32**, 969 (1985).
- <sup>15</sup>K. Murase and T. Fukunaga, in *Optical Effects in Amorphous Semiconductors*, edited by P. C. Taylor and S. G. Bishop, AIP Conf. Proc. No. **120** (AIP, New York, 1984), p. 449.
- <sup>16</sup>Z. V. Popovic, M. Holtz, K. Reimann, and K. Syassen, *Phys. Status Solidi B* **198**, 337 (1996).